Modeling and Experimental Study of an Ammonia-water Falling Film Absorber

Delphine Triché, Sylvain Bonnot, Maxime Perier-Muzet, François Boudéhenn, Hélène Demasles, Nadia Caney

Available online at www.sciencedirect.com

ScienceDirect

Energy Procedia 91 (2016) 857 – 867

Energy Procedia

SHC 2015, International Conference on Solar Heating and Cooling for Buildings and Industry

Modeling and experimental study of an ammonia-water falling film absorber

Delphine Triché [a,b,c,*], Sylvain Bonnot[a], Maxime Perier-Muzet[a], François Boudéhenn[a], Hélène Demasles[a], Nadia Caney[b]

[a]CEA LITEN INES, 50 avenue du Lac Léman, 73375 Le Bourget du Lac, France
[b]Univ. Grenoble Alpes, LEGI, F-38000 Grenoble, CNRS, LEGI, F-38000 Grenoble, France
[c]Agence de l'Environnement et de la Maîtrise de l'Energie 20, avenue du Grésillé - BP 90406 49004 Angers Cedex 01, France

Abstract

This paper presents a numerical and experimental study of absorption phenomenon in ammonia-water absorption chiller which is a very promising technology in the solar cooling field. The purpose of the research is to analyse the coupled heat and mass transfers that take place in a plate heat exchanger used as absorber in order to identify limiting transfers. For this purpose, a numerical modeling of a falling film absorber has been performed. Then, an experimental study has been carried out on a test bench in order to experiment the absorber in real operating conditions and to validate the numerical model. So, experimental and numerical results are compared to discuss hypothesis of the model and analyse the global behaviour of the absorber. Moreover, local phenomena are discussed thanks to the numerical study.

Peer-review by the scientific conference committee of SHC 2015 under responsibility of PSE AG

Keywords: falling film absorber; ammonia-water; numerical model; experimental results

1. Introduction

In the current context of air conditioning democratization, it is important to find an alternative to vapour compression chillers which are supposed to represent approximately 99% of the today's sold units. Indeed, since the

* Corresponding author. Tel.: +33-479-792-340; fax: +33-479-792-303.
E-mail address: delphine.triche@cea.fr

Peer-review by the scientific conference committee of SHC 2015 under responsibility of PSE AG
doi:10.1016/j.egypro.2016.06.252

beginning of the 2000s, these machines have led to an important increase in electricity consumption and greenhouse gas emissions [1]. An alternative could be the use of ammonia-water absorption chillers which generate cooling effect by using environment friendly refrigerant and are thermally driven. However, these machines have to be improved to become competitive, in terms of design, of operative behaviour and finally of cost.

Mittermaier and Ziegler [2] have shown that the overall performance of the absorption process is determined by the absorber. Indeed, global performance of the chiller is impacted by low efficiency of the absorber heat and mass transfer process. As a result, the absorber is one of the most critical components of the absorption chiller in terms of size, cost and efficiency, so it is necessary to understand its behaviour in order to improve global performances of the chiller.

Over the last years, many numerically and analytically studies have been performed about the absorption process in ammonia water absorption chillers in order to predict heat and mass transfer in absorber. For example, Goel and Goswami [3] studied a counter current absorber using a finite difference method and empirical correlations for transfer coefficients to understand coupled transfers, Gommed and al [4] used finite volume method to quantify the absorption process and Cerezo [5] studied a bubble absorber using a one-dimensional model in order to estimate absorption fluxes and absorption coefficients.

In a review article dedicated to numerical studies of falling film absorber, Killion and Garimella [6] have pointed out that for ammonia-water working fluid most of the authors neglect mass transfer resistances in vapour phase (considered as pure ammonia) or in liquid phase. In the present work, mass transfer resistances in both liquid and vapour phases are considered to discuss where the limiting mass transfer resistance is.

Regarding experimental studies, most of them are not performed in real operating conditions. Indeed, some test benches dedicated to the absorption process allow the study of the absorber but the behaviour of the absorber is uncoupled of the behaviour of the global absorption chiller. For example, Kang and al [7] experimentally studied ammonia-water falling film absorption process comparing the effect of various operating conditions on heat and mass transfer performances: the method enables operating conditions to vary but absorber is tested without taking account of global chiller behaviour.

In the present work, a low cooling capacity (5 kW) prototype of ammonia-water absorption chiller has been used to study the absorber behaviour in real operating conditions. This prototype was built in 2010 and numerous previous tests proved its capacity to maintain steady-state conditions. Studied absorber is a commercial plate heat exchanger used as absorber. This technology has been chosen because of its compactness and its low cost.

Therefore, the purpose of this study is to analyse the absorber behaviour, particularly heat and mass flows inside it, in order to predict its performances.

Nomenclature

A	Transfer area	$[m^2]$
c	Correction coefficient	[-]
Cp	Heat capacity	$[J.kg^{-1}.K^{-1}]$
δ	Boundary layer thickness	[m]
dAi	Interfacial area of the differential control volume	$[m^2]$
ΔL	Length of the differential control volume	[m]
Exp	Experimental	
h	Heat transfer coefficient	$[W.m^{-2}.K^{-1}]$
H	Specific Enthalpy	$[J.kg^{-1}]$
$\tilde{H}$	Partial enthalpy	$[J.kg^{-1}]$
K	Mass transfer coefficient	$[m.s^{-1}]$
λ	Thermal conductivity	$[W.m^{-1}.K^{-1}]$
L	Length of the absorber	[m]
$\dot{m}$	Mass flow rate	$[kg.s^{-1}]$
N_{NH3}	Surface mass flux of ammonia absorbed or desorbed at the interface	$[kg.m^{-2}.s^{-1}]$
N_{H2O}	Surface mass flux of water absorbed or desorbed at the interface	$[kg.m^{-2}.s^{-1}]$

Np	Number of plates	
Num	Numerical	
P	Pressure	[Pa]
Q	Heat transfer	[W]
ρ	Density	[$kg.m^{-3}$]
T	Temperature	[K]
U	Global heat transfer coefficient	[$kW.m^{-2}.K^{-1}$]
x	Mass fraction of ammonia in the liquid phase	[-]
y	Mass fraction of ammonia in the vapour phase	[-]
z	Mass fraction of ammonia in the absorbed or desorbed flux	[-]

Subscripts

A	Absorber
abs	Absorbed
L	Liquid
V	Vapour
C	Coolant fluid
C	Condenser
E	Evaporator
film	Falling film
G	Generator
in	Inlet
int	Interface
out	Outlet
P	Plate
R	Rectification exchanger
SENL	Sensible liquid
SENV	Sensible vapour

2. Method

2.1. Experimental device description

The experimental study has been performed on a prototype of a low cooling capacity (5 kW) ammonia-water absorption chiller (Fig. 1) designed for solar applications. The prototype of the chiller is composed of 7 plate heat exchangers: the generator, the absorber, the evaporator, and the condenser; a solution heat exchanger located between rich and poor solution; a subcooler located between the liquid refrigerant at the inlet of the evaporator and the vapour refrigerant at the outlet of the evaporator; and a rectification exchanger.

Four tanks are used to perform liquid-vapour separation, for storage or for control. A pump is used to transfer solution from absorber to generator. And finally, two electronic expansion valves are used to control the chiller.

The studied absorber is a corrugated plate heat exchanger with 16 plates: 8 channels are supplied with coolant fluid and 7 channels are supplied with liquid solution and vapour. Therefore, there are 14 falling films (Fig. 2).

It is a co-current falling film absorber that means that refrigerant vapour flows in the same direction as the solution (from the top to the bottom). However, the coolant fluid flows in counter-current with the falling film, that is mean that coolant enters at the bottom of the absorber. Geometric dimensions of the absorber are summarized in Table 1.

This chiller is fully instrumented with temperature, pressure and liquid level sensors and Coriolis flow meters. Thanks to this instrumentation, it is possible to calculate the mass fraction of ammonia of the absorber's inlet and

outlet flows (poor solution, rich solution and vapour). Instruments also enable to know the coolant temperature and the coolant mass flow rate at the bounds of the absorber. The sensors are quantified and described in Table 2.

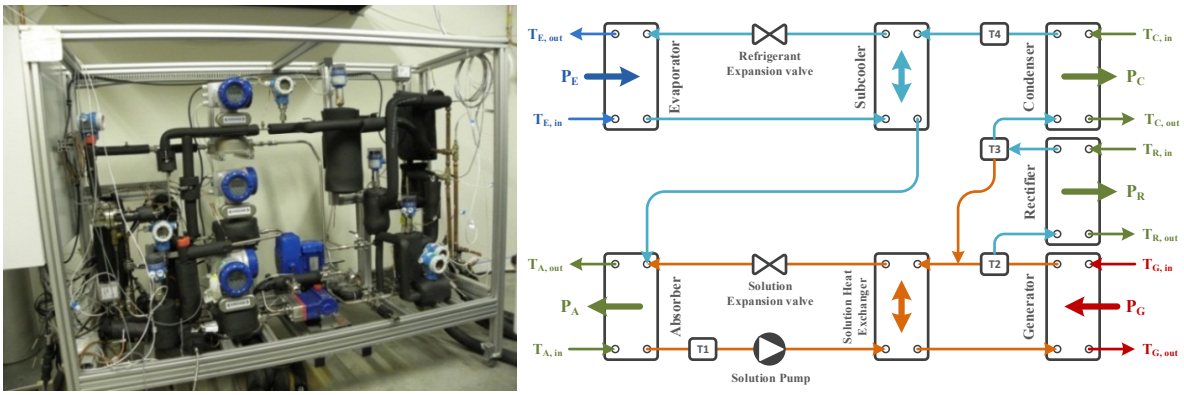

Fig. 1. Prototype of ammonia-water absorption chiller (left) and architecture of the chiller (right).

Table 1. Geometric dimensions of the absorber.

Cooling plate type	Corrugated plates
Cooling plate material	Alloy 316
Cooling plate width	111 mm
Cooling plate length	526 mm
Cooling plate thickness	0.4 mm
Number of cooling plates	16
Spacing between two adjacent cooling plates	2 mm

Table 2. Sensors number and measurement characteristics.

Sensors type	Number	Uncertainty (+/-)
Coolant fluid temperature (Pt)	10	0.1 K
Refrigerant and solution temperature (TC)	15	0.3 K
Refrigerant pressure (0-10bar and 0-25bar)	4	0.2 %
Coriolis flow meters:	3	
- Mass flow rate		0.1 % *Manufacturer uncertainty
- Density		2 kg/m^3

Pt: Platinum resistance thermometer, TC : Thermocouple

External fluid temperatures, rich solution and coolant mass flow rates are control parameters used to modified the operating conditions of the chiller in order to perform the sensibility analysis of the absorber.

2.2. Numerical model description

A numerical model of the absorber has been developed in order to study combined heat and mass transfers in the falling film plate absorber. The model is a one dimension model which allows the iterative resolution of nonlinear equations in each differential control volume of the absorber Fig. 2.

To compare numerical results with experimental results, two simulations have been realized. On the first hand, a simulation has been performed on an edge plate and on the second hand another simulation has been carried out on a central plate. These two numerical simulations allow the calculation of mass flow rates, concentration and temperature using masses, species and energies balances at the absorber outlet mixing point.

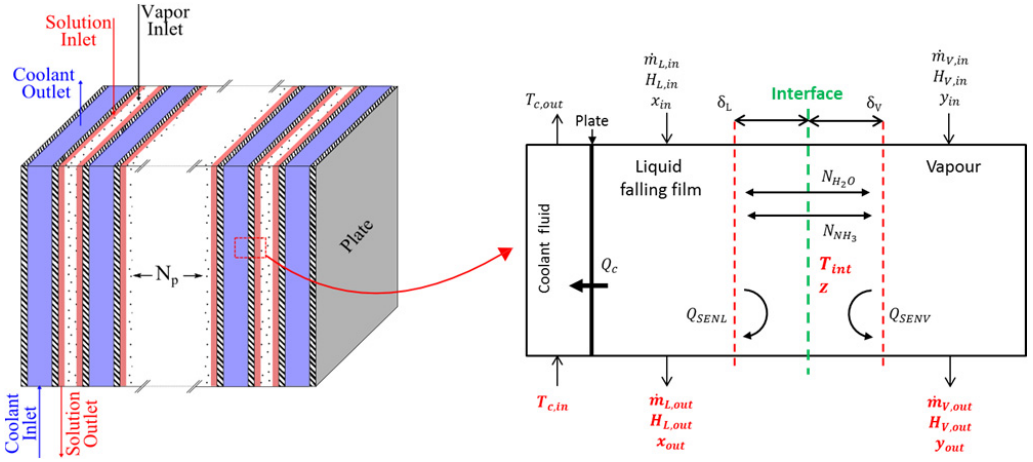

Fig. 2. Diagram of the absorber (left), Differential control volume of the absorber (right).

Mass transfer resistances in both liquid and vapour phases are considered because water is a volatile absorbent which is present in the two phases. Transport phenomena are thus much complex compared to any other currently used fluid pair as water and lithium bromide (a non-volatile absorbent) [6]. Several assumptions have been made to establish the model:

- Absorption process is in steady state;
- Pressure is homogenous in the absorber;
- Solution at the vapour/solution interface is considered saturated;
- Plates of the heat exchanger are assumed to be flat plates;
- Exchange surface is totally wet (there is no direct exchange between the vapour phase and the coolant fluid);
- There are no heat exchange with the environment through the absorber walls;
- Temperatures of liquid phase and vapour phase in each control volume are assumed to be mixing temperatures;
- Vapour at the input of the absorber is assumed to be a saturated vapour;
- Liquid falling films are laminar;
- Flow rates distribution is equal in all channels of the absorber;
- Effect of non-absorbable gases is ignored;
- Longitudinal conductions inside the plates and inside the fluids are considered negligible.

The mathematical model is based on mass balances, species balances, energy balances, mass and heat transfer equations and equilibrium conditions at the vapour/solution interface for each control volume [8]. Empirical correlations are used to predict heat and mass transfer coefficients. Main model equations are presented in the following section.

Mass balances, in the vapour phase (1) and in the liquid phase (2) are:

$$\dot{m}_{V,in} - \dot{m}_{V,out} - (N_{NH3} + N_{H2O}).dAi = 0 \quad (1)$$

$$\dot{m}_{L,in} - \dot{m}_{L,out} + (N_{NH3} + N_{H2O}).dAi = 0 \quad (2)$$

Species balances, in the vapour phase (3) and in the liquid phase (4) are:

$$\dot{m}_{V,in}.y_{in} - \dot{m}_{V,out}.y_{out} - N_{NH3}.dAi = 0 \quad (3)$$

$$\dot{m}_{L,in}.x_{in} - \dot{m}_{L,out}.x_{out} + N_{NH3}.dAi = 0 \quad (4)$$

N_{NH3} and N_{H2O} are the surface mass fluxes of ammonia or water absorbed or desorbed at the interface between liquid and vapour phases. Positives values imply a mass transfer from vapour to liquid (absorption) and negatives values imply a mass transfer from liquid to vapour (desorption).

Energy balance in the vapour phase (5) is:

$$-Q_{SEN_V} + \dot{m}_{V,in}.H_V(T_{V,in}, P, y_{in}) - \dot{m}_{V,out}.H_V(T_{V,out}, P, y_{out}) - N_{NH3}.H_{V,NH3}(T_{int}, P).dAi - N_{H2O}.H_{V,H2O}(T_{int}, P).dAi = 0 \quad (5)$$

The ammonia-water mixed vapour is considered as a perfect ideal gas mixture, so partials enthalpies are equal to pure component enthalpy ($H_{V,NH3}$ and $H_{V,H2O}$)

Energy balance in the liquid phase is (6):

$$-Q_{SEN_L} - Q_C + \dot{m}_{L,in}.H_L(T_{L,in}, P, x_{in}) - \dot{m}_{L,out}.H_L(T_{L,out}, P, x_{out}) + N_{NH3}.\widetilde{H}_{L,NH3}(T_{int}, P).dAi + N_{H2O}.\widetilde{H}_{L,H2O}(T_{int}, P).dAi = 0 \quad (6)$$

$\widetilde{H}_{L,NH3}$ and $\widetilde{H}_{L,H2O}$ are partials enthalpies of ammonia and water in the liquid phase.

The solution at the vapour/solution interface is considerate saturated; therefore, the equilibrium mass fractions of ammonia at the interface can be expressed by saturation equations.

Energy balance at the interface between liquid and vapour phases (7) is:

$$N_{NH3}.\left(\widetilde{H}_{V,NH3}(T_{NH3,V}, P) - \widetilde{H}_{L,NH3}(T_{NH3,L}, P)\right).dAi + N_{H2O}.\left(\widetilde{H}_{V,H2O}(T_{H2O,V}, P) - \widetilde{H}_{L,H2O}(T_{H2O,L}, P)\right).dAi + Q_{SEN_L} + Q_{SEN_V} = 0 \quad (7)$$

$Q_{SEN\,V}$ is sensible heat exchanged between the vapour phase and the interface and $Q_{SEN\,L}$ is sensible heat exchanged between the liquid phase and the interface.

When heat and mass transfers are coupled at the interface of a liquid phase and a vapour phase, an extra quantity of heat is transferred due to the heat capacity of mass transfer. So, $Q_{SEN\,V}$ (8) and $Q_{SEN\,L}$ (9) are expressed by:

$$Q_{SEN_V} = \frac{c_V}{1-e^{-c_V}}.h_V.dAi.(T_V - T_{int}) \quad (8)$$

$$Q_{SEN_L} = \frac{c_L}{1-e^{-c_L}}.h_L.dAi.(T_L - T_{int}) \quad (9)$$

With:

$$c_V = \frac{N_{NH3}.Cp_{V,NH3} + N_{H2O}.Cp_{V,H2O}}{h_V} \quad (10)$$

$$c_L = \frac{N_{NH3}.Cp_{L,NH3} + N_{H2O}.Cp_{L,H2O}}{h_L} \quad (11)$$

Mass diffusion and bulk transport of ammonia and water across the liquid-vapour interface imply mass transfer between the liquid and the vapour phase [3].

The total mass flux which is transferred between vapour and liquid-vapour interface is expressed by (12):

$$N_{NH3} + N_{H2O} = K_V . \rho_V . \ln\left(\frac{z - y_{int}}{z - y}\right) \quad (12)$$

The total mass flux which is transferred between liquid-vapour interface and liquid phase is expressed by (13):

$$N_{NH3} + N_{H2O} = K_L . \rho_L . \ln\left(\frac{z - x}{z - x_{int}}\right) \quad (13)$$

z is the mass fraction of ammonia in the absorbed/desorbed flux. It is expressed as follows (14):

$$z = \frac{N_{NH3}}{N_{NH3} + N_{H2O}} \quad (14)$$

The liquid mass transfer coefficient K_L is calculated with an empirical correlation developed by Yih and Chen [9]. This correlation is only valid in a falling film with a Reynolds number between 49 and 300 and in fully developed conditions. The vapour heat transfer coefficient h_V is calculated with an empirical correlation [10]. The vapour mass transfer coefficient K_V and the liquid heat transfer coefficient h_L are determined by the Chilton and Colburn analogy [11].

To evacuate the heat of the absorption process, the coolant fluid absorbs an amount of heat which is calculated with an energy balance in the coolant fluid (15):

$$Q_C + \dot{m}_C . \left(H_{C,in} - H_{C,out}\right) = 0 \quad (15)$$

With:

$$Q_C = U . dAi . (T_L - T_{C,in}) \quad (16)$$

U is the global heat transfer coefficient which takes into account both convective transfers (between falling film and plate and between coolant fluid and plate) and conduction across the plate. Correlation used to calculate the global heat transfer coefficient U has been expressed by Goel and Goswami [3].

In this study, thermodynamic properties are calculated with the software REFPROP which allows the calculation of several fluids and mixtures properties and more particularly ammonia-water mixture properties [12]. Transport properties are predicted using Conde Engineering correlations [13].

Based on these equations a simulation tool has been developed with the Scilab software. As a result, the numerical model provides thermodynamic properties (T, P, $\dot{m}$, H, x, y) and transport properties along the absorber plate. It is thus possible to analyse heat and mass flows through the liquid vapour interface, to facilitate the study of the absorption process and to analyse the absorber 7ehavior to predict and enhance its performances.

3. Results and discussion

The diagram of the differential control volume of the absorber numerically studied is presented in Fig.2 and geometric dimensions of this absorber are summarized in Table 1.

3.1. Global analysis of the absorber

Experimental tests have been realized on the absorber with several operating conditions. These tests enable to analyse the 7ehavior of the absorber with variation of its inlets flow conditions. These experimental test conditions

have been used as input data to perform numerical simulations in order to carry out a comparison between numerical and experimental results. The operating conditions of the 4 experiments considered for this study are listed in Table 3. Table 4 summarizes results obtained experimentally and numerically and allows the comparison.

Table 3. Operating conditions at the inlet of the absorber.

Tests	$\dot{m}_{V,in,exp}$ [kg/s]	$\dot{m}_{L,in}$ [kg/s]	$T_{V,in}$ [K]	$T_{L,in}$ [K]	x_{in} [-]	$y_{in,exp}$ [-]	$y_{in,sat\ vap}$ [-]	P [Pa]	$T_{C,in}$ [K]	$\dot{m}_C$ [kg/s]
1	$5{,}25.10^{-3}$	$1{,}67.10^{-2}$	296,9	312,0	0,460	0,995	0,999	$6{,}03.10^{5}$	300,2	0,326
2	$4{,}89.10^{-3}$	$2{,}26.10^{-2}$	287,8	317,0	0,494	0,993	0,9999	$6{,}09.10^{5}$	300,2	0,325
3	$4{,}95.10^{-3}$	$2{,}25.10^{-2}$	293,6	317,1	0,493	0,989	0,9997	$6{,}08.10^{5}$	300,2	0,325
4	$5{,}52.10^{-3}$	$2{,}19.10^{-2}$	293,0	314,6	0,484	0,991	0,9997	$6{,}01.10^{5}$	299,1	0,325

Table 4. Comparison of the results at the outlet of the absorber.

Tests	$\dot{m}_{V,out}$ [kg/s]		$T_{L,out}$ [K]		$\dot{m}_{L,out}$ [kg/s]		x_{out} [-]		$\dot{m}_{V,abs}$ [kg/s]		$T_{C,out}$ [K]		Q_C [W]	
	Exp	Num	Exp	Num	Exp	Num	Exp	Num	Exp	Num	Exp	Num	Exp	Num
1	0	$6{,}72.10^{-5}$	303,7	303,7	$2{,}22.10^{-2}$	$2{,}23.10^{-2}$	0,591	0,597	$5{,}25.10^{-3}$	$5{,}64.10^{-3}$	305,8	306,4	7,76	7,86
2	0	$5{,}8.10^{-5}$	303,5	304,1	$2{,}78.10^{-2}$	$2{,}80.10^{-2}$	0,588	0,593	$4{,}89.10^{-3}$	$5{,}49.10^{-3}$	305,5	306,7	7,61	7,87
3	0	$5{,}63.10^{-5}$	304,0	304,1	$2{,}78.10^{-2}$	$2{,}80.10^{-2}$	0,588	0,593	$4{,}95.10^{-3}$	$5{,}48.10^{-3}$	305,8	306,7	7,71	8,05
4	0	$6{,}74.10^{-5}$	303,0	303,2	$2{,}78.10^{-2}$	$2{,}79.10^{-2}$	0,591	0,595	$5{,}52.10^{-3}$	$5{,}98.10^{-3}$	305,1	306,0	8,39	8,69

The decrease of the temperature of the falling film along the absorber indicates a good cooling of the liquid. The relation between the absorbed vapour and the liquid flow rates at the inlet of the absorber shows a good absorption process.

Comparison between experimental and numerical results in terms of temperature, mass flow rate and concentration in the liquid solution at the outlet of the absorber shows a good agreement since a maximal relative error of 1 % is observed. Vapour mass flow rates at the outlet of the absorber should be zero to make sure of the complete absorption of the vapour phase but in the numerical study it just approach zero to assure the stability of the model. Regarding the absorbed mass flow rate, numerical results are superior to experimental ones, that is mean that absorption process is overestimated in the numerical study. This more important absorption process implies an amount of heat absorbs in the coolant fluid superior in the numerical study compared to the experimental one.

Experimental mass balance is not correct even if the manufacturer uncertainty is considered (Table 2). This error may be due to a higher measurement uncertainty or an unsteady flow. Other tests will be performed to analyse this problem.

3.2. Detailed analysis of numerical results

As mentioned earlier, the developed numerical model provides temperature, mass flow and NH_3 mass fraction profiles along the absorber length. Mass fluxes of ammonia or water absorbed or desorbed can also be obtained. All masses, species and energies balances and heat and mass transfer equations are solved with residual errors lower than1.10^{-7}. Profiles presented in the following section are profiles in central channels.

Fig. 3. presents the variation of temperatures along the absorber. The heat transfer fluid cools the absorption process by flowing counter-current with the falling film. As a result the liquid solution temperature (T_L) decreases along the absorber and the coolant fluid temperature (T_C) increases. The interface temperature (Tint) is always slightly higher than the liquid solution temperature because of the absorption heat generated at the interface. Vapour phase temperature (T_V) strongly increases at the top of the absorber and reaches interface temperature at an absorber

length of 289 mm. Once the interface temperature is reached, heat transfers are reversed and vapour temperature decreases with liquid and interface temperatures.

Fig. 4. shows the evolution of ammonia mass fractions along the absorber. As explained before, z represents the ammonia mass fraction in the absorbed/desorbed flux. If z is superior to 1, water is desorbed from liquid to vapour and if z is inferior to 1, water is absorbed from vapour to liquid. The interface vapour (y_{int}) and the interface liquid (x_{int}) ammonia mass fractions increase along the absorber because of the decreasing of interface temperature. Moreover, vapour ammonia mass fraction (y) decreases when z is higher than vapour concentration and increases when z is lower than vapour concentration. Finally, all along the absorber, ammonia mass fraction of liquid solution (x) increases because of the high concentration of the absorbed flux compared to the liquid phase one.

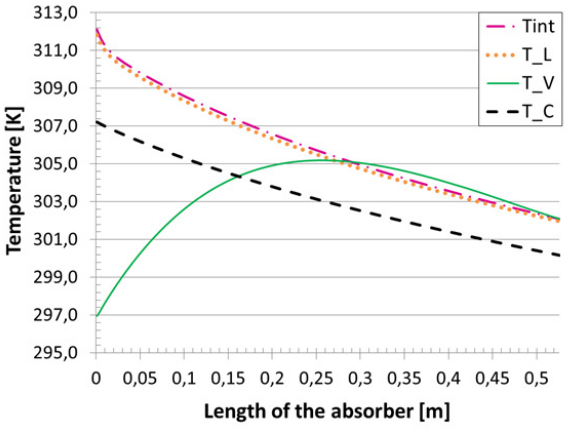

Fig. 3. Profile of temperatures along the absorber.

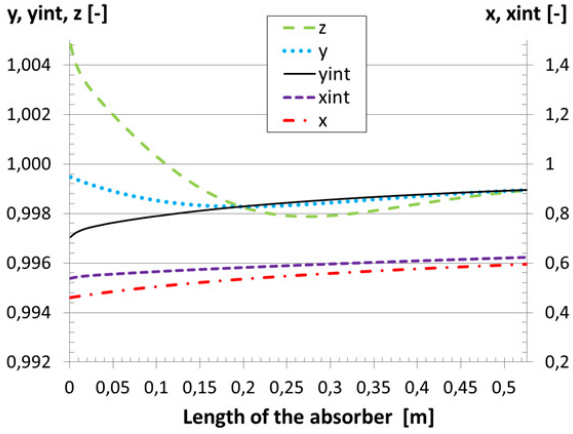

Fig. 4. Variation of ammonia mass fraction along the absorber.

Fig. 5. shows the variation of exchanged mass fluxes along the absorber. Positive value of the ammonia mass flux indicates absorption of ammonia from vapour to liquid. Negative and positive values of the water mass flux indicate firstly desorption of water from liquid to vapour and secondly absorption of water from vapour to liquid.

Fig.6. illustrates the change of mass flow rates along the absorber. The vapour phase mass flow rate decreases along the absorber because vapour is absorbed in the liquid phase. Therefore, liquid phase mass flow rate increases. The value of the vapour mass flow rate at the outlet of the absorber should approach zero to make sure of the complete absorption of the vapour phase.

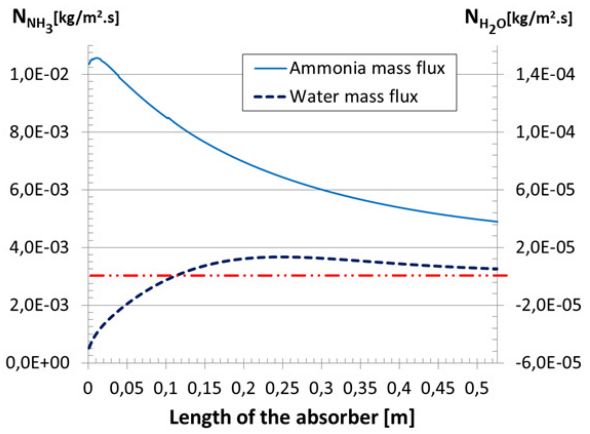

Fig. 5. Profile of absorbed /desorbed fluxes along the absorber.

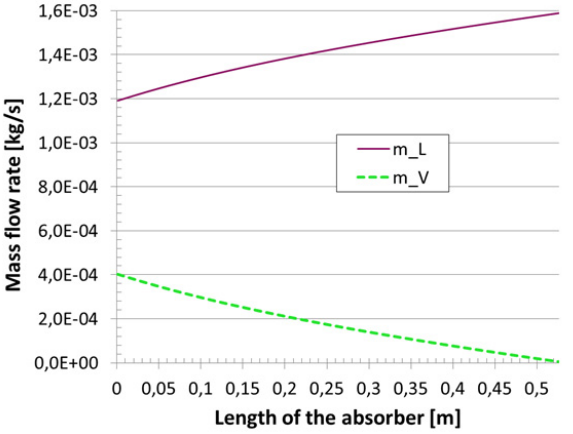

Fig. 6. Variation of mass flow rates along the absorber.

This simulation results allows also a more detailed analysis of local phenomena. Firstly, at the top of the absorber, z is superior to 1 and superior to ammonia mass fraction in the vapour phase; moreover, ammonia mass fraction in the vapour phase is higher than ammonia mass fraction at vapour interface; therefore water is desorbed by diffusion process, ammonia is absorbed and ammonia mass fraction in vapour phase decreases. The high temperature of liquid phase implies low absorption of ammonia and high desorption of water by diffusion process. Then, liquid phase temperature decreases strongly because of the difference between coolant temperature and liquid phase one; therefore, absorption of ammonia increases and desorption of water decreases.

Then, z decreases and becomes lower than 1 because of the decreasing of liquid temperature; so water is now absorbed from vapour phase to liquid phase and other flows behaviour remains identical.

After that, vapour ammonia mass fraction becomes lower than interface vapour ammonia mass fraction and z becomes lower than vapour ammonia mass fraction. This phenomenon is due to the decrease of the difference between y and x. The absorbed mass flux being less concentrated than the vapour phase, ammonia mass fraction increases in the vapour phase and ammonia and water are always absorbed in the liquid phase.

Finally, once vapour temperature reaches liquid temperature at the bottom of the absorber, the absorbed water mass flux decreases and z increases.

4. Conclusion

An experimental study of a falling film plate heat exchanger absorber has been carried out on a fully instrumented absorption chiller prototype and a numerical study has been performed in parallel to analyse local phenomena. The absorption chiller prototype enables to test the absorber in real operating conditions and to validate the model. The numerical study will enable to simulate other operating conditions and geometric dimensions.

Observed differences can be explained by assumptions made to establish the model. However, although several assumptions have been used (flat plates, fully developed flows), numerical results are close to experimental ones on the first tests performed.

To study the absorber in more detail, other experiments will be performed on this absorber. Then a new absorber which has different corrugated plates and which will be more instrumented will be studied. These new tests should validate hypothesis to finally allow a better sizing of the absorber necessary to improve performances of the global chiller.

References

[1] Pons M, Anies G, Boudéhenn F, Bourdoukan P, Castaing-Lasvignottes J and al. Performance comparison of six solar-powered air-conditioners operated in five places. Energy 2012;46:471–83.
[2] Mittermaier M, Ziegler F. Theoretical evaluation of absorption and desorption processes under typical conditions for chillers and heat transformers. International Journal of Refrigeration 2015.
[3] Goel N, Goswami DY. Analysis of a counter-current vapor flow absorber. International Journal of Heat and Mass Transfer 2005;48:1283-92
[4] Gommed K, Grossman G, Koenig M. Numerical study of absorption in a laminar falling film of Ammonia-Water. ASHRAE 2001.
[5] Cerezo J, Bourouis M, Vallès M, Coronas A, Best R. Experimental study of an ammonia-water bubble absorber using a plate heat exchanger for absorption refrigeration machines. Applied thermal engineering 2009;29:1005-11.
[6] Killion JD, Garimella S. A critical review of models of coupled heat and mass transfer in falling-film absorption. International Journal of refrigeration 2001;24:755-97
[7] Kang YT, Akisawa A, Kashiwagi T. Experimental correlation of combined heat and mass transfer for NH3-H2O falling film absorption. International Journal of refrigeration 1999;22:250-62.
[8] Kang YT, Christensen RN. Development of a counter-current model for a vertical fluted tube GAX absorber. International absorption Heat Pump Conference 1993;31.
[9] Yih SM, Chen KY. Gas absorption into wavy and turbulent falling liquid films in a wetted-wall column. Chemical Engineering Communications, 1982;17:123-36.
[10] Taylor R, Krishna R. Multicomponent Mass Transfer, John Wiley & Sons, 1993.
[11] Chilton TH, Colburn AP. Mass Transfer (Absorption) Coefficients, Industrial and Engineering Chemistry 1934;26:1183-87.
[12] Tillner-Roth R, Friend DG. Survey and assessment of available measurements on thermodynamic properties of the mixture "Water-Ammonia". J. Phys. Chem. Ref. Data 1998;27:45-61.
[13] Conde M. Thermophysical properties of ammonia-water mixtures for the industrial Design of Absorption Refrigeration Equipment, M. CONDE Engineering, 2006.